# Dynamic Mechanical Properties and Structure of *In Situ* Cured Polyurethane/Hydrogenated Nitrile Rubber Compounds: Effect of Carbon Black Type

**Urška Šebenik,[1] József Karger-Kocsis,[2] Matjaž Krajnc,[1] Ralf Thomann[3]**

[1]*Faculty of Chemistry and Chemical Technology, University of Ljubljana, Aškerčeva cesta 5, SI-1001 Ljubljana, Slovenia*
[2]*Polymer Engineering, Faculty of Mechanical Engineering, Budapest University of Technology and Economics, H-1111 Budapest, Hungary*
[3]*Institut für Makromolekulare Chemie und Freiburger Materialforschungszentrum, Albert-Ludwigs-Universität Freiburg, Stefan-Meier-Strasse 31, D-79104 Freiburg, Germany*

Received 20 May 2011; accepted 11 September 2011
DOI 10.1002/app.35626
Published online 20 December 2011 in Wiley Online Library (wileyonlinelibrary.com).

**ABSTRACT:** A peroxide-curable hydrogenated nitrile rubber (HNBR) was modified by *in situ* crosslinked polyurethane (PU) in a 1 : 1 weight ratio. PU was formed from solid PU precursors, polyester polyol, and blocked polyisocyanate incorporated in the HNBR during the curing of the latter. HNBR/PU blends containing carbon black (CB) of different types (N234, N330, and N550) were prepared in this work. Thirty parts of CB per hundred parts of polymer matrix (HNBR and PU) were used. The curing of PU was followed by differential scanning calorimetry (DSC). Information of the phase structure was derived from DSC and dynamic mechanical analysis (DMA) tests. DMA results suggested that a quasi-interpenetrating network structure developed in the HNBR/PU blend. This was confirmed also by scanning electron microscopy, transmission electron microscopy (TEM), and atomic force microscopy inspections. The partition of CB between the PU and HNBR was assessed by TEM. It was established that CB was exclusively located in the HNBR phase. CB N234 proved to be more efficient reinforcement than N330 and N550. © 2011 Wiley Periodicals, Inc. J Appl Polym Sci 125: E41–E48, 2012

**Key words:** atomic force microscopy (AFM); interpenetrating networks (IPN); polyurethanes; reinforcement; rubber

## INTRODUCTION

Polyurethane (PU) is probably the most versatile polymer with respect to its synthesis, processing, properties, and applications. This also makes PU an interesting candidate for blending with rubbers. However, blending with rubbers requires PU to be available in a millable (i.e., rubberlike) or solid form. The few works that have dealt with PU/rubber blends used thermoplastic,[1–5] decomposed crosslinked PUs[6–8] or millable (peroxide- or sulfur-crosslinkable) PU rubbers.[9,10] Because of the fact that PU precursors are overwhelmingly liquids (i.e., both polyisocyanate and polyol are liquids), researchers have paid less interest to the production of PU/rubber combinations with these urethane precursors.[11] On the other hand, a large body of work has been devoted to PU/rubber systems containing ground and crumb waste rubbers. Research and development in the past has overlooked a further possibility that underlines the versatile synthesis of PUs: PU precursors are also available in solid form, which enables their blending with various rubbers in the traditional way. Solid PU precursors contain crystalline polyols and blocked polyisocyanates. The deblocking of the polyisocyanates occurs at a temperature ($T$) higher than the melting of the polyol and results in an *in situ* formed PU. It is noteworthy that the deblocking temperature is close to that of the usual curing temperature of rubbers. The combination of curable rubbers with *in situ* crosslinkable PU from its solid precursors has a further important feature: the crosslinking reactions are running parallel; that is, they are practically not influenced by each other. The PU formed may have a thermoplastic or thermoset nature, depending on the functionalities of the precursors. Solid precursors of *in situ* crosslinkable PUs are on the market, especially for demanding adhesive applications.

Recently, we have shown that this new blending concept is straightforward. The related works have focused on the wear behavior of PU/ethylene–propylene–diene (EPDM)[12] and PU/hydrogenated nitrile rubber (HNBR) combinations.[13] The major outcome of these works has been that the performance of PU/rubber combinations depends on the compatibility of the blend components and the presence of

*Correspondence to:* J. Karger-Kocsis (karger@pt.bme.hu).

reinforcing fillers. HNBR has proven to be a more suitable blending component with PU than EPDM. One can improve the wear resistance and mechanical properties of PU/EPDM blends by filling them with carbon black (CB). The partition of CB between the blend components, on the other hand, may have a strong impact on the mechanical properties. Moreover, a CB partition may also effect the phase separation of the blend components.

The aim of this work was to produce blends of peroxide-curable HNBR and *in situ* crosslinkable PU from a solid precursor and to study their structure-related thermomechanical performance as a function of CB type. The HNBR/PU ratio and the CB amount were fixed at 1 : 1 and 60 parts per hundred of HNBR (30 parts per hundred of polymer matrix), respectively. The selected HNBR/PU ratio resulted in an interpenetrating network (IPN) structure. The IPN is the most sensitive structure for compositional changes and, thus, represents a suitable model system for studying the effect of CB on the phase structure of the blends. A further aim of this work was to study the reinforcing effect achieved by CBs of different activities added in the same amounts.

## EXPERIMENTAL

### Material and sample preparation

As a PU precursor, Nolax HCM 555-D (particle size $<$ 200 μm, Nolax AG, Sempach-Station, Switzerland) was used; it is marketed as a one-component, hot-melt PU adhesive. This PU was composed of a crystalline polyol and a blocked polyisocyanate compound.

The composition of the peroxide-curable HNBR was as follows: HNBR {Therban LT VP/KA 8882, Lanxess, Leverkusen, Germany, acrylonitrile content = 21%, Mooney viscosity ML[1 + 4)100°C = 74]} = 100 parts, diphenylamine-based thermostabilizer (Luvomaxx CDPA, Lehmann & Voss, Hamburg, Germany) = 1.1 phr (part per hundred parts of rubber), zinc-containing mercaptobenzimidazole compound (Vulcanox ZMB 2/C5, Lanxess) = 0.4 phr, di(*t*-butylperoxyisopropyl) benzene (Perkadox 14–40 B-PD, Akzo-Nobel, Düren, Germany; active peroxide content = 40%) = 7.5 phr, MgO = 2 phr, triallyl isocyanurate = 1.5 phr, and ZnO = 2 phr. This base mix was produced separately and was provided by Lanxess. The curing time of the base mix to reach 90% crosslinking was about 10 min at 175°C.

The peroxide-curable HNBR was mixed with the PU precursor in a 1 : 1 weight ratio on a two-roll mixing mill (LRM-150BE, Labtech, Bangkok, Thailand) at ambient temperature with a friction ratio of 1.15. The HNBR/PU mixes were also prepared with CB loading. The CB content was constant, 30 parts of CB per hundred parts of polymer matrix (HNBR and PU) were used. On the other hand, CBs with different reinforcing activities and, thus, different primary particle sizes were selected: N234, N330, and N550 (Zaozhuang Xinyuan Chemical Industry Co., Zaozhuang, China). According to the related standard (ASTM D 2516), the primary mean particle size ranges of N234, N330, and N550 CBs are 24–33 nm (intermediate superabrasion furnace), 28–36 nm (high abrasion furnace), and 39–55 nm (fast extruding furnace), respectively.

The peroxide-curable HNBR, HNBR/PU blend, and HNBR/PU/CB compounds were cured at 175°C for 10 min in a laboratory press. The curing conditions were chosen in accordance with those needed to reach optimum curing of HNBR. For comparison purposes, plain PU sheets were also produced under identical curing conditions from the PU precursor. Specimens for the investigations listed in the following text were cut from compression-molded sheets about 2 mm thick.

### Thermal properties and curing of PU

The thermal properties and curing of the PU precursor were assessed by differential scanning calorimetry (DSC). The measurements were performed on a Mettler-Toledo DSC821e instrument (Schwerzenbach, Switzerland) with an intracooler and STAR$^e$ software. Octane, In, and Zn standards were used for the temperature calibration and for the determination of the instrument time constant. A nitrogen atmosphere and standard 40-μL alumina pans were used. The sample mass was about 20 mg. A DSC method with five segments was applied. The alumina pan containing the PU sample was inserted onto the DSC sensor at −120°C and left at −120°C for 5 min to allow the sample to reach the cell temperature. First, a heating run from −120 to 70°C and a cooling run back to −120°C were performed to erase the thermal history of the sample. Then, by a heating run from −120 to 240°C, the thermal properties and curing of the PU precursor were monitored. The heating to 240°C was followed by a cooling back to −120°C. A last heating run from −120 to 350°C allowed us to investigate the thermal properties of the cured PU, its degree of curing, and its thermal stability. The heating and cooling rates of the dynamic segments were 10 and −10°C/min, respectively.

### Phase structure and compatibility

The parent rubber (HNBR), PU, and their blend with and without 30 phr CB of various types were subjected to DSC and dynamic mechanical analysis (DMA) measurements.

DSC measurements of the cured rubber blends were performed with the DSC apparatus described previously. In this case, a DSC method with a temperature program, which could be compared to a DMA method, was chosen. The alumina pan containing a sample was inserted onto the DSC sensor at room temperature and cooled to −120°C. When the sample reached −120°C, the first heating run from −120 to 100°C was started. The first heating was followed by a cooling segment from 100 to −120°C and a subsequent second heating run from −120 to 200°C. The heating and cooling rates were 10 and −10°C/min, respectively.

The dynamic mechanical properties were measured in shear mode on a DMA861[e] instrument (Mettler-Toledo). The samples were prepared in a disc shape (ca. 1.8 mm thick and with a radius of about 5 mm). A linearity check was carried out, and the measurements were performed within the linear viscoelastic regime. The dynamic mechanical properties were recorded at constant frequencies of 1, 2, 5, and 10 Hz as a function of the temperature (from −70 to 80°C) with a constant heating rate 2°C/min.

The phase structure of the blends and the CB dispersion within the polymer matrix were studied by scanning electron microscopy (SEM), transmission electron microscopy (TEM), and atomic force microscopy (AFM). SEM pictures of cryomicrotomed sections of the specimens were taken by an FEI Quanta 250 field emission gun (FEG) device (FEI, Hillsboro, OR). Cryocutting was done at −120°C by a Diatome (Biel, Switzerland) diamond knife with a Leica EM UC6 ultramicrotome (Leica Mikrosysteme, Wetzlar, Germany) equipped with a cryochamber. The corresponding cut surfaces were inspected at an acceleration voltage of 5 kV without sputtering with a high-resolution low-voltage high-contrast backscatter electron detector (vCD). The TEM device (Zeiss LEO 912 Omega, Zeiss Oberkochen, Germany) was operated at acceleration voltage of 120 kV. Thin specimens (thickness ≈ 50 nm), prepared by cryocutting with the aforementioned ultramicrotome at −120°C, were subjected to TEM investigations without any staining. AFM experiments were performed with a Nanoscope III scanning probe microscope (Digital Instruments, Santa Barbara, CA). The height and phase images were obtained simultaneously while the instrument was operated in the tapping mode under ambient conditions. Images were taken at the fundamental resonance frequency of the Si cantilevers, which was typically around 300 kHz. Typical scan speeds during recording were 0.3–1 lines per second with scan heads with a maximum range of 50 × 50 $\mu m^2$. The phase images represented the variations of the relative phase shifts (i.e., the phase angle of the interacting cantilever relative to the phase angle of the freely oscillating cantilever at the resonance frequency) and were thus able to distinguish materials by their material properties (e.g., filler and polymer). The flat surfaces of the samples examined were obtained by cryocutting, as described previously.

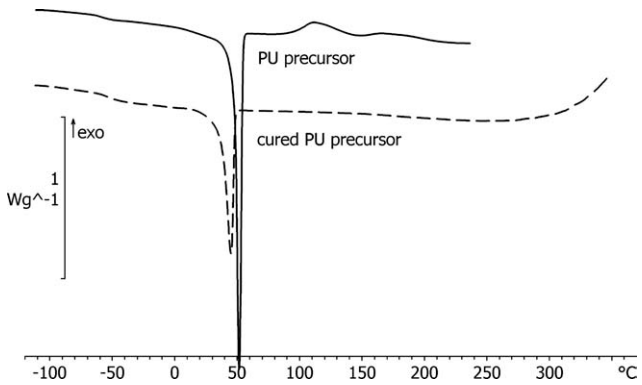


**Figure 1** DSC thermograms of the PU precursor (first heating) and resulting cured PU (second heating). The thermal degradation of the cured PU started at about 300°C, that is, far beyond the curing temperature of the HNBR/PU mixes.

## RESULTS AND DISCUSSION

### PU curing

In Figure 1, DSC thermograms of the PU precursor (heating run from −120 to 240°C) and the resulting cured PU (heating run from −120 to 350°C) are shown. The thermogram of the PU precursor showed a glass-transition temperature ($T_g$) at $T \approx -60$°C and an endothermic peak at $T \approx 50$°C, which was due to the melting of polyol segments. This endothermic peak was followed by an exothermic signal with two peaks at $T \approx$ 115 and 165°C, respectively. The occurrence of two exothermic signals was attributed to two chemical reactions: the deblocking of the —NCO groups and the reaction between the —OH and —NCO groups.[12] After curing, the melting peak for the polyol segments, built in the cured PU, occurred at $T \approx 45$°C. $T_g$ of the crosslinked PU was at $T \approx -50$°C, whereas its decomposition started at $T \approx 270$°C.

The DSC thermogram showing the curing of the HNBR/PU mix (Fig. 2) differed significantly from that of the PU precursor. The crosslinking reactions, likely superimposed on one another, started at $T \approx$ 140°C and ran at a maximum rate at $T \approx 190$°C. The DSC thermogram in Figure 2, however, substantiates that adequate conditions (i.e., 10 min at 175°C) were chosen for the curing of the blends.

### Glass transitions of the cured rubber blends

Figure 3 displays the DSC thermograms of cured plain HNBR and PU, HNBR/PU blend, and HNBR/PU/CB

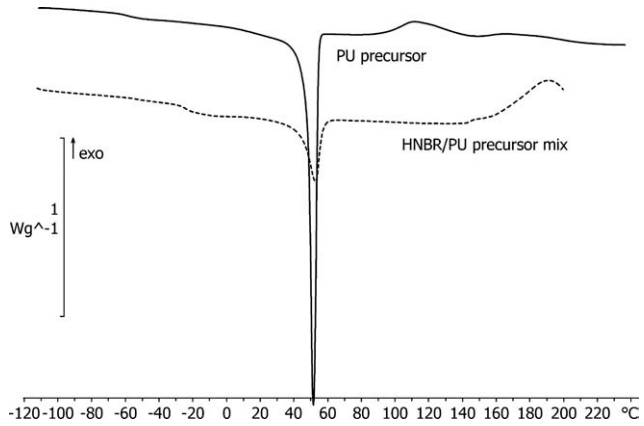


**Figure 2** DSC thermograms showing the curing of the PU precursor and HNBR mixed with the PU precursor.

compounds in the $T_g$ range. One can recognize that the $T_g$ of PU ($T_g \approx -50°C$) was lower than that of HNBR ($T_g \approx -35°C$). Two $T_g$'s were also resolved for the cured HNBR/PU blend, although there was a shift in the $T_g$ of HNBR toward higher temperatures ($T_g \approx -20°C$). This may have been linked with interchain crosslinking, as proposed for PU/HNBR by Maity et al.[10] The $T_g$ of HNBR in the HNBR/PU/CB compounds shifted back to that of the plain HNBR with decreasing reinforcing activity of CB (N234 $\gg$ N330 > N550). This suggested that the surface chemistry of CB may have affected the possibility of interchain crosslinking. The $T_g$ step of PU in the HNBR/PU/CB compounds could be resolved only at high magnification of the heat flux; by contrast, the melting peak of the polyol soft segments remained in the same temperature range.

## DMA behavior

Figure 4 shows the DMA traces [storage shear modulus ($G'$) and loss factor (tan δ) as a function of temperature] of the HNBR, PU, and HNR/PUR blend at 1 Hz. At this frequency, HNBR had a $T_g$ at −22°C, whereas PU had a $T_g$ around −30°C when we considered the position of the related tan δ peaks. The sharp $G'$ decrease for PU at temperatures between 40 and 55°C was related to the melting of the soft polyol segments, as discussed previously. Recall that this transition was also prominent in the DSC curves of PU (Figs. 1 and 2). The DMA curves of the HNBR/PU blend exhibited characteristics of incompatible blends. In the tan δ versus $T$ trace, the $T_g$ related to HNBR at $T_g \approx -13°C$ (peak) could be identified, whereas the glass transition of PU could be identified as a shoulder (of the same peak) at lower temperatures, where the PU curve also exhibited a broad peak. Note that the $T_g$ of HNBR in the HNBR/PU blend was shifted toward higher temperatures. The most probable reason for the $T_g$ shift was a phase-structure-induced constraint. Interestingly, the melting of the soft phase of PU was markedly reduced in the HNBR/PU blend (Fig. 2). This shift was associated with a change in the onset of the melting-related transition, which for the HNBR/PU blend, occurred at lower temperatures (Fig. 4). Its appearance may have been an effect of the dipole–dipole interactions between —CN groups of HNBR and —OH groups of PU, which hampered the crystallization of the polyol segments in PU.[12]

$G'$ of PU was below that of HNBR at temperatures where HNBR was in a glassy state. On the other hand, a combination of HNBR and PU yielded a synergistic effect with respect to $G'$ below the $T_g$ of HNBR. This may have been due to some constraint effect arising in the IPNs. The $G'$ versus $T$ curves of the HNBR/PU blend reflected the $T_g$ of the HNBR component and the melting of the PU segments. By contrast, the $T_g$ effect of PU on the $G'$ versus $T$ behavior of the blend was less obvious. This supported, again, the assumption of a constrained phase structure, most likely in IPN form. The $G'$ versus $T$

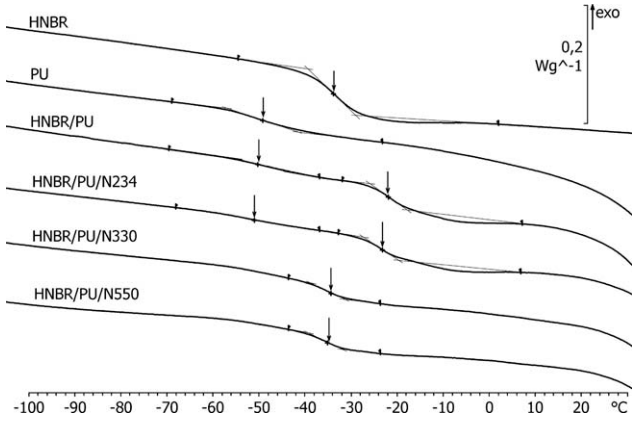


**Figure 3** DSC thermograms of the cured HNBR, PU, HNBR/PU blend, and HNBR/PU/CB compounds with different CB types in the $T_g$ range.

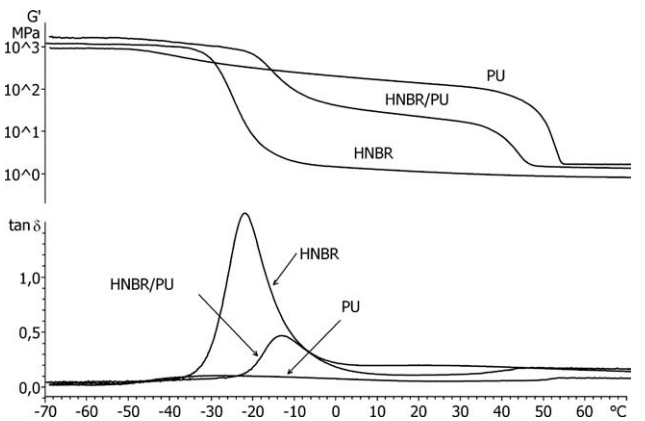


**Figure 4** Temperature dependence of $G'$ and tan δ of the HNBR, PU, and HNBR/PU blend at 1 Hz.

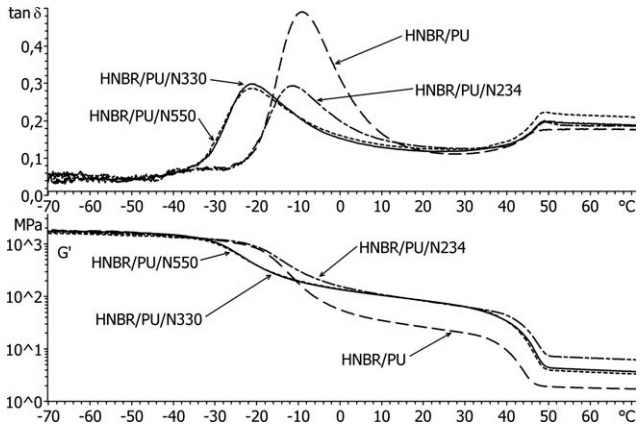


**Figure 5** Temperature dependence of $G'$ and tan δ of the HNBR/PU blend with and without 30 phr CB of different types at 10 Hz.

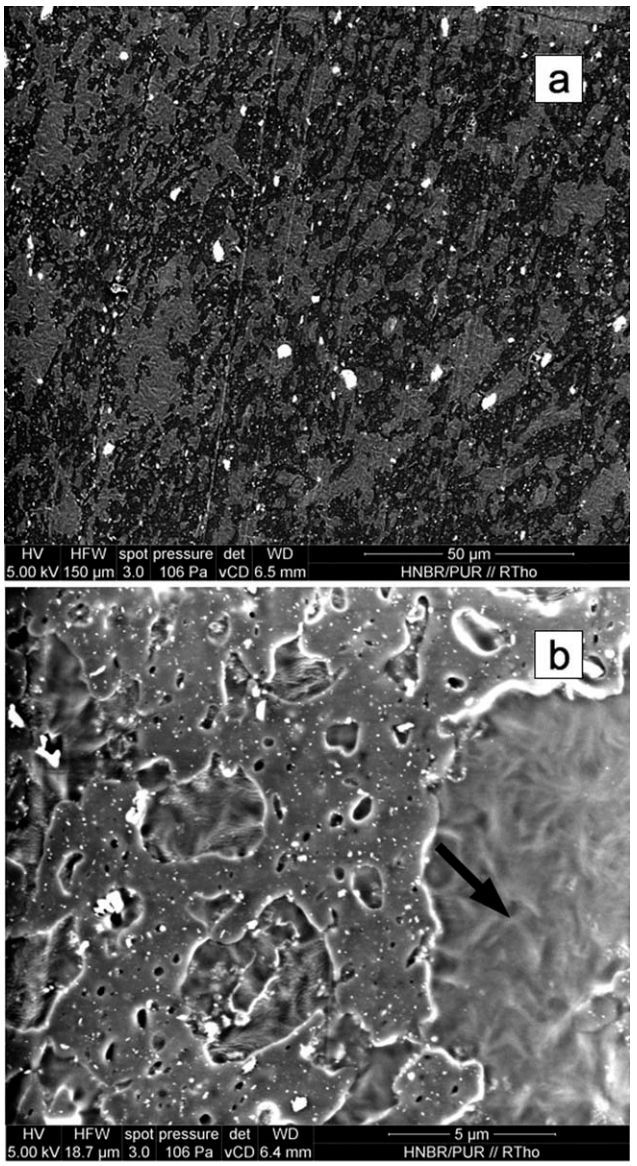


**Figure 6** SEM pictures taken from the cryocut surface of the HNBR/PU blend at various magnifications.

trace of HNBR/PU was between those of the parent rubber and PU; this further hinted at the presence of an IPN-like structure.

Figure 5 displays the $G'$ versus $T$ and tan δ versus $T$ traces for the HNBR/PU blend and different HNBR/PU/CB compounds at 10 Hz. The effects of the use of less active CBs (N330 and N550) on the properties ($G'$ vs $T$ and tan δ vs $T$ traces) of the resulting compounds (HNBR/PU/N330 and HNBR/PU/N550) were very similar. On the other hand, the compound with highly active CB (HNBR/PU/N234) behaved differently. A common aspect of all of HNBR/PU/CB compounds was that the intensity of the $T_g$ relaxation peak of HNBR (on the tan δ curve) was strongly reduced, whereas that of the PU did not change. This suggested that CB was preferentially located in the HNBR phase. The most striking effect in the tan δ versus $T$ traces was a big change in the position of the HNBR $T_g$ because of the different CB activity and related changes in the phase structure. In the presence of CBs N330 and N550, the HNBR $T_g$ was below that of the HNBR/PU blend, whereas when CB N234 was added, the HNBR $T_g$ agreed with that of the parent blend. This was a clear hint that some characteristics of the phase structure (supposed as IPN-like) were influenced by the CB type and activity. The $G'$ values of all of the HNBR/PU/CB compounds were higher than those of the parent HNBR/PU blend above the HNBR glass transition (Figs. 4 and 5). The runs of the $G'$ versus $T$ traces of the HNBR/PU/CB compounds with N330 and N550 were practically

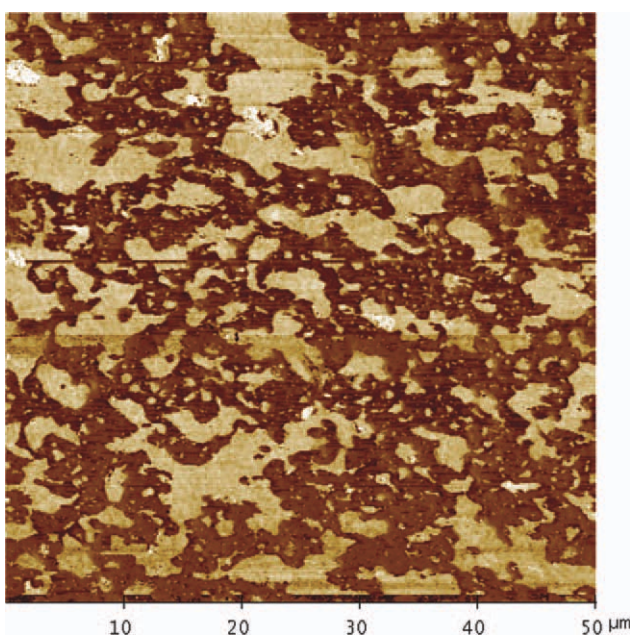


**Figure 7** AFM phase image of the HNBR/PU blend. The dark and white phases represent HNBR and PU, respectively. [Color figure can be viewed in the online issue, which is available at wileyonlinelibrary.com.]

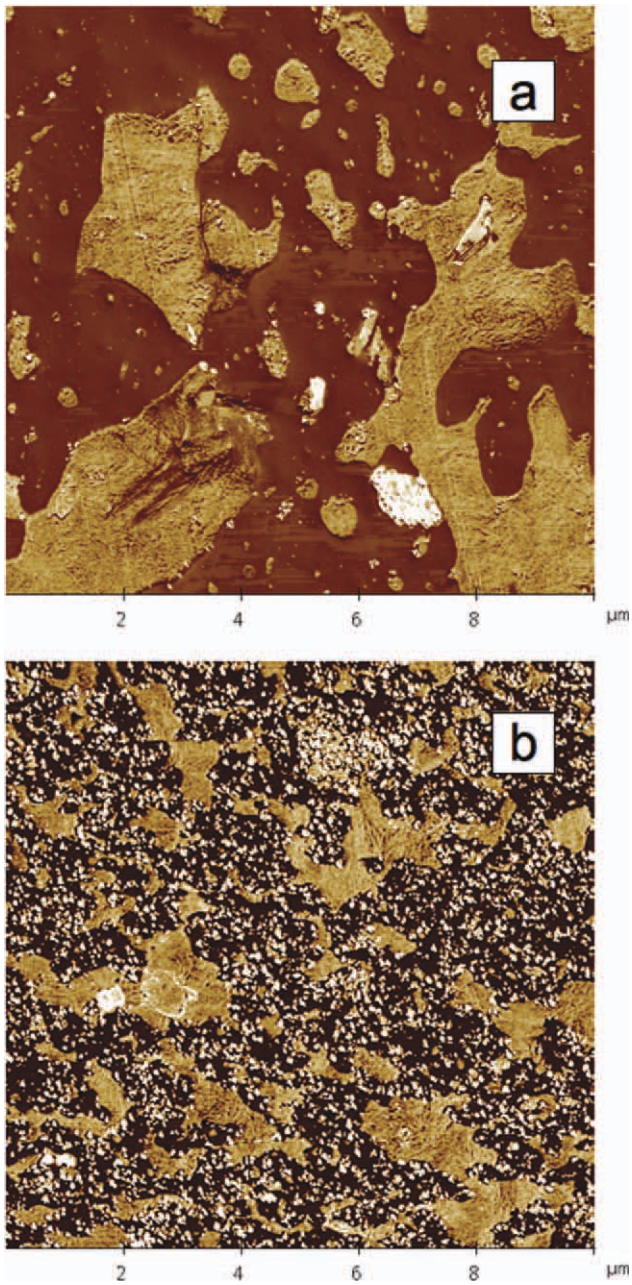


**Figure 8** AFM phase images of the HNBR/PU blend (a) without and (b) with 30 phr CB N330 (HNBR/PU/N330). The dark and white phases represent HNBR and PU, respectively. [Color figure can be viewed in the online issue, which is available at wileyonlinelibrary.com.]

identical in the whole temperature range studied. When the compound contained N234, the modulus dropped because the glass transitions and melting occurred at higher temperatures. Between 10 and 35°C, the $G'$ values were the same for all of the HNBR/PU/CB systems, regardless of the CB type. However, the CB type affected the plateau moduli above the melting of the polyol segments of PU ($T >$ 50°C). Moreover, the plateau moduli reflected well the activity of CB according to the expected ranking: N550 < N330 ≪ N234.

## Phase structure

SEM pictures taken of the cut surface of the HNBR/PU blend are given in Figure 6. The low-magnification SEM picture suggested the presence of an IPN-like structure [Fig. 6(a)], whereas at high magnification, the crystalline structure of PU turned out very clearly [Fig. 6(b)]. The lamellar crystalline structure of PU is indicated by an arrow.

The IPN-like structure of HNBR/PU was also confirmed by AFM (Fig. 7).

The incorporation of CB affected the fine structure of the IPN as the mean domain size of PU was markedly reduced. This is well represented by the AFM pictures in Figure 8. Moreover, the AFM images in Figure 8 demonstrate that CB was embedded exclusively in the HNBR phase. This could be traced to the following: high filler uptake by the amorphous HNBR, filler exclusion due to the highly crystalline PU, and better wetting of CB by HNBR than by PU due to surface energetic issue.

The lamellar structure of the crystalline PU phase was well resolved at high magnification (Fig. 9). This AFM image also evidences that CB was located in the dark HNBR phase.

The preferential location of CB in HBNR was also confirmed by TEM results. Figure 10(a) displays that the CB N330 could only be found in the HNBR phase. The high-magnification TEM picture in Figure 10(b) shows the sizes of the CB particles, aggregates, and agglomerates. One can see that the average primary particle size of CB was about

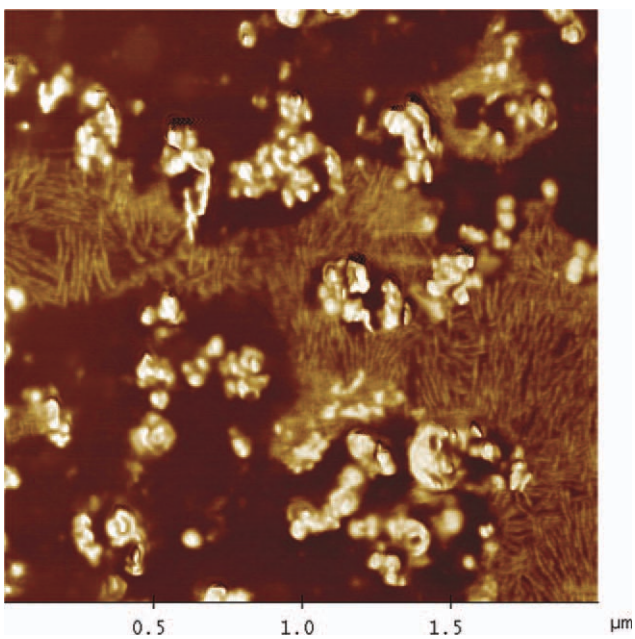


**Figure 9** AFM phase image of the HNBR/PU/N550 compound containing 30 phr N550 CB. [Color figure can be viewed in the online issue, which is available at wileyonlinelibrary.com.]

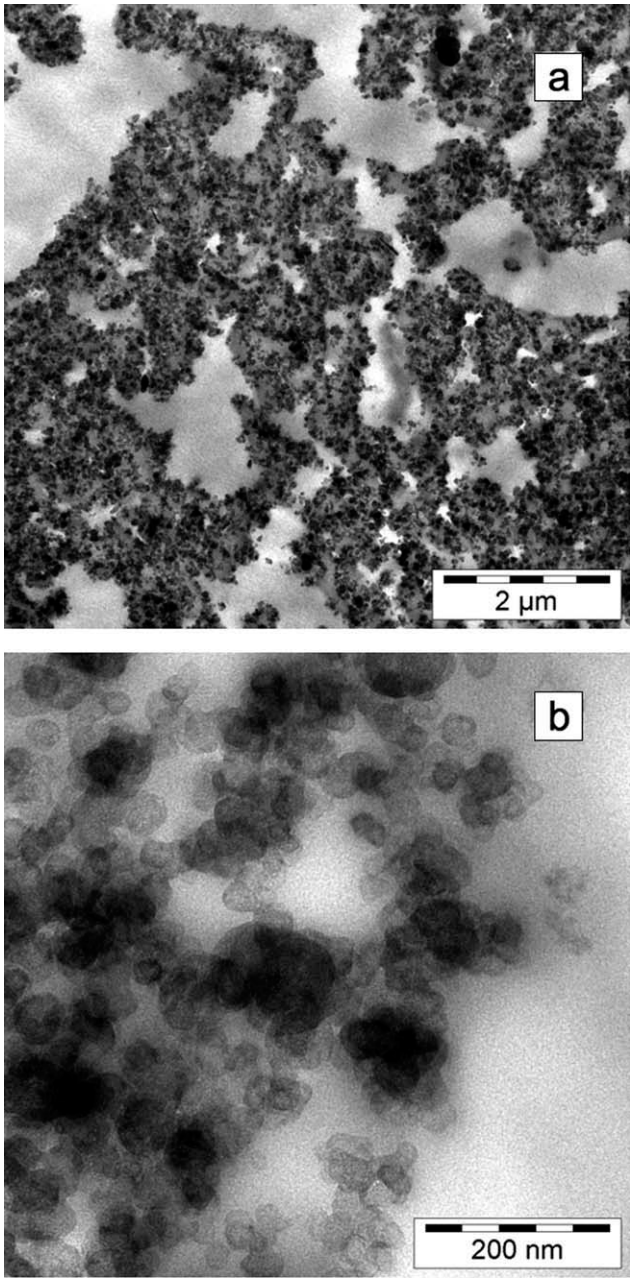


**Figure 10** TEM pictures of the HNBR/PU/N330 compound reinforced by 30 phr CB N330 at different magnifications.

30 nm, which was in accordance with the grading of the CB N330 according to ASTM D 2516.

The morphology results thus proved the suggestions derived from the DSC and DMA results: that the HNBR/PU blend was incompatible, that both phases were likely continuous in the 1 : 1 blend, that CB was exclusively embedded in HNBR, and that its incorporation influenced the fine structure of IPN accompanied with different levels of morphological constraint. This is the right place to draw attention to the fact that the parent IPN-like structure was on the micrometer scale instead of the nanoscale (or molecular scale). Prerequisite of interlacing in the latter case is linked with some compatibility of the blend components, which was lacking for the HNBR/PU combination. It is well known, however, that incompatible thermoplastic blends may exhibit a cocontinuous structure,[14] especially at a composition ratio of 1/1. When this phase structure is stabilized in a suitable way (additives, interfacial reaction, etc.), it does not turn into a dispersed one during blending but remains cocontinuous on a micrometer scale. Something similar happened in our case. The separate crosslinking of the HNBR and PU components strongly contributed to the preservation of the cocontinuity. Nonetheless, as no ultimate evidence was delivered on the IPN structuring of the HNBR/PU blends, the terms *IPN-like* and *quasi-IPN* are used.

## CONCLUSIONS

This work was devoted to the production of a novel hybrid rubber through the blending of peroxide-curable HNBR with a solid PU precursor (polyol and blocked polyisocyanate) with *in situ* curing during the crosslinking of HNBR. The blends were reinforced with CBs of different activity. The thermal and dynamic mechanical properties of the corresponding compounds were studied, and their phase structure was concluded from SEM, AFM, and TEM investigations. The results can be summarized as follows:

- HNBR/PU blends with a 1 : 1 composition with and without CB, added in 30 phr amount, were successfully produced. The blend components were incompatible, as shown by DSC and DMA results. The latter suggested the structuring of the blend components as an IPN.
- The quasi-IPN structure was confirmed by the SEM, AFM, and TEM studies. The CB added was exclusively incorporated into the HNBR phase. CB incorporation affected the fine structure of the IPN and caused differences in the morphological constraint.

This work was performed in the framework of the following projects: bilateral cooperation between Hungary and Slovenia (BI-HU/10-11-009). Part of this work was also linked with the project "Development of Quality-Oriented and Harmonized R + D + I Strategy and Functional Model at BME," which was supported by the New Hungary Development Plan (project ID TÁMOP-4.2.1/B-09/1/KMR-2010-0002).

## References

1. Dhamodharan, R.; Maiti, P.; Radhakrishnan, G. Polym Plast Technol Eng 2007, 46, 163.
2. Tan, J.; Ding, Y. M.; He, X. T.; Liu, Y.; An, Y.; Yang, W. M. J Appl Polym Sci 2008, 110, 1851.

3. Wang, X.; Luo, X.: Eur Polym J 2004, 40, 2391.
4. Wu, L.; Luo, X.; Wang, X. J Appl Polym Sci 2006, 102, 5472.
5. Šebenik, U.; Poljanšek, I.; Krajnc, M. E-Polymers 2006, no. 041.
6. Gremmels, J.; Ishiaku, U. S.; Mohd Ishak, Z. A. Kautsch Gummi Kunstst 2000, 53, 528.
7. Mousa, A.; Karger-Kocsis, J. Plast Rubber Compos 2001, 30, 309.
8. Radhesh Kumar, C.; Karger-Kocsis, J. Eur Polym J 2002, 38, 2231.
9. Singha Roy, S. K.; Das, C. K. Polym Polym Compos 1995, 3, 403.
10. Maity, M.; Khatua, B. B.; Das, C. K. Int J Polym Mater 2001, 49, 407.
11. Desai, S.; Thakore, I. M.; Brennan, A.; Devi, S. J Macromol Sci Pure Appl Chem 2001, 38, 711.
12. Karger-Kocsis, J.; Felhös, D.; Xu, D. Wear 2010, 268, 464.
13. Xu, D.; Karger-Kocsis, J. J Appl Polym Sci 2010, 115, 1651.
14. Pötschke, P.; Paul, D. R. J Macromol Sci Polym Rev 2003, 43, 87.